Optimizing Repair Welding Techniques in Cast Steels—Part II

H_2-induced cracking can be prevented by using low hydrogen practice if the maximum HAZ hardness is below Rc 35, and all steel castings should be normalized before repair welding

BY D. K. AIDUN AND W. F. SAVAGE

ABSTRACT. Four different heats of cast steel were used for hydrogen-induced cracking studies using low- and high-hydrogen practice in simulated repair welds. It was shown that to prevent hydrogen-induced cracking where good low-hydrogen practice is not possible, the maximum "safe" level of hardness in the heat-affected zone should be below Rc 35.

Metallographic examination of these cast-steel weldments showed seven distinct regions from the fusion zone out toward and including the unaffected base metal. These regions are:

1. Fusion zone.
2. Unmixed zone.
3. Coarse-grained homogeneous HAZ.
4. Fine-grained homogeneous HAZ.
5. Partially transformed region.
6. Spheroidized region.
7. Unaffected base metal.

All as-cast heats with carbon contents ranging from 0.21 to 0.32 wt-%, upon exposure to a 5-second arc time, exhibited maximum hardness levels of about 70 Rc in the networks of martensite surrounding the islands of untransformed ferrite in the partially transformed region. This was attributed to the inhomogeneity of the as-cast structure. However, for low-carbon cast steels this problem was eliminated by normalizing the alloy before the welding operation. For cast steels of about 0.30 wt-%, in addition to homogenization, a postweld heat treatment would be advisable.

Introduction

It is generally recognized that four requisites must be met simultaneously for hydrogen-induced cracking to occur. These can be summarized as follows:

1. *A metallurgical requisite.* For cracking to occur, a crack-sensitive microstructure must be present, and, in general, the susceptibility to hydrogen-induced cracking increases with increase in the hardness of the microstructure.

2. *A chemical requisite.* For cracking to occur, the level of diffusible hydrogen present in the crack-susceptible microstructure must exceed a critical concentration, which decreases sharply as the yield strength of the microstructure present increases (Ref. 1).

3. *A mechanical requisite.* Although cracking has been shown to initiate at lower stress levels, it appears that crack propagation requires localized stresses of approximately yield-strength magnitude (Ref. 2).

4. *An environment requisite.* Hydrogen-induced cracking has been shown to result from the extraordinary reduction in the notched-tensile strength of steels caused by the presence of a relatively small amount of diffusible hydrogen (Ref. 3). Since this loss in strength in the presence of a notch occurs only in the range −148 to 390°F (−100 to 200°C), hydrogen-induced cracking requires that the weldments be exposed to temperatures within this range in the presence of the first three requisites.

Although in theory hydrogen-induced cracking can be prevented by elimination of any one of the above requisites, in practice it is usually possible to exert control over only the first two. This results from the fact that the thermally-induced residual stresses in all but the simplest of weldment geometries are usually sufficient in magnitude to initiate cracking if the other requisites are met. Furthermore, unless stress relief heat treatment is performed after welding, the addition of service usually raises the localized stresses in the weldment above the critical level for crack propagation.

Because most welded structures experience service in the crack-sensitive temperature range, this requisite is usually met. However, it is possible to take advantage of this requirement in two ways:

1. *Postweld soaking.* It has been shown by Adams (Ref. 4) and others that an immediate postweld soak for 30 minutes (min) to one hour (h) at a temperature of above 390°F (200°C) will usually prevent hydrogen-induced cracking. This is attributed mainly to the reduction in the level of diffusible hydrogen made possible by the greatly increased diffusivity of hydrogen at 390°F (200°C). Thus, by the time the weldment is allowed to return to the crack-sensitive temperature range, the residual level of diffusible hydrogen is rendered below the critical level for crack initiation.

2. *Cryogenic storage.* In conducting laboratory studies, it is convenient to be able to store welded specimens under conditions which preclude either loss of hydrogen or the formation of hydrogen-induced cracks until controlled experiments can be initiated. This has been shown (Ref. 5) to be possible by transfer of the weldments to liquid nitrogen (−320°F) (−195.8°C boiling point) as soon as they reach ambient temperature and storing under liquid nitrogen until the experiments begin.

The critical hardness level is influenced

D. K. AIDUN is Assistant Professor, Mechanical and Industrial Engineering Department, Clarkson University, Potsdam, New York; and W. F. SAVAGE is Professor Emeritus, Rensselaer Polytechnic Institute, Troy, New York.

Table 1—Chemical Composition, Initial Hardness (IH), and Ideal Critical Diameter (D_I) of Heat 32, 27, 1, and 0

	Composition, wt-%			
	32	27	1	0
C	0.32	0.31	0.21	0.26
Mn	1.15	1.57	1.24	0.74
P	0.017	0.013	0.018	0.021
S	0.017	0.013	0.031	0.028
Si	0.54	0.50	0.51	0.40
Ni	–	0.03	0.07	0.04
Cr	0.13	0.14	0.20	0.31
Mo	0.22	0.10	0.03	0.02
Cu	0.04	0.04	0.04	0.03
Al	0.078	0.054	0.11	0.075
IH, Rc	51	51	46	48
D_I, in.	3.17	3.51	2.05	1.61

by the toughness and ductility of the microstructure of the weld heat-affected zone (HAZ). Of the various possible microconstituents, untempered martensite is the most brittle and, therefore, the most susceptible to hydrogen-induced cracking. The other microconstituents, listed in order of decreasing susceptibility, include lower bainite, upper bainite, pearlite, spheroidite, and ferrite.

In general, the toughness and ductility both of individual and particular combinations of microconstituents is decreased by increasing the carbon content of the prior austenite. For this reason, the susceptibility to hydrogen-induced cracking is directly related to the carbon content of the steel. For a given carbon content, increasing the percentage of martensite in the weld heat-affected zone lowers the critical hydrogen concentration required to cause hydrogen-induced cracking.

Carbon is the least expensive of all alloying elements. Because of this, steel foundries tend to increase the carbon content of their steels in order to achieve higher strength. The increase in carbon content increases the ideal critical diameter, D_I, more than any other alloying element; in addition, it also increases the hardness of any martensite formed.

A few years ago, the railroad industry began to investigate the failure of cast components such as couplers, yokes, and knuckles. As a result of this investigation, it was concluded that hydrogen-induced cracking was a contributing cause of failure. It seemed likely that hydrogen-induced cracking could result from improper welding procedures used in repairing casting defects in these structures. It was suspected that, in the absence of suitable control of repair-welding procedures, crack susceptible heat-affected-zone microstructures could easily be produced.

Unfortunately, repair welds in steel castings are often performed solely for "cosmetic" reasons to eliminate superficial surface imperfections. The rapid cooling rates, which are associated with such "cosmetic" repairs, coupled with inadequate control of sources of hydrogen such as improper handling and storage of consumables, greatly increase the probability of hydrogen-induced cracking.

Underbead cracking is one of the most insidious forms of hydrogen-induced cracking. This is because it often is located entirely beneath the weld and fails to emerge at the surface where it can be detected by nondestructive inspection. Unfortunately, the geometry of most repair welds is such as to make this a dominant form of hydrogen-induced cracking in steel castings. If undetected, such cracks may experience slow crack growth in service until the critical crack size is reached and catastrophic failure occurs.

Materials and Specimen Preparation

Four heats of cast steel were used in this investigation. Table I lists the chemical composition, initial hardness, IH (the hardness of martensite), and ideal critical diameter, D, (based upon 50% martensite), for all four heats.

The four heats, supplied in the form of cast coupons, had dimensions that were approximately 10¼ × 4¼ × ¾ in. (260 × 108 × 19 mm). From these coupons, specimens of 10 × 2 × ½ in. (254 × 50.8 × 13 mm) were machined for the hydrogen-induced cracking test. The surface on which the welds were to be deposited was then polished with 240 grit SiC paper and degreased with acetone.

Polishing and degreasing are critical and important for the hydrogen-induced cracking test when using low-hydrogen welding practice. These cleaning operations mitigate hydrogen absorption in the weld by removing hydrogenous materials from the surface of the specimen.

Procedure

The electrode type, hydrogen content, heat treatments, and the heats of steel used in this part of the investigation are summarized in Table 2. The level of diffusible hydrogen in welds was measured by the RPI silicone-oil extraction technique (Ref. 6). Two levels of diffusible hydrogen were studied:

1. Low-hydrogen practice. After removal from hermetically sealed shipping containers, the electrodes were transferred immediately to a well-ventilated holding oven and maintained at 350°F (177°C) until just before use. This procedure gave an average level diffusible hydrogen of approximately 3 ppm (3.3 cc/100 g of weld metal).

2. High-hydrogen practice. The electrodes were removed from the open shipping container, dipped in water for 30 s and used immediately. This practice gave an average diffusible hydrogen level of 30 ppm (33.3 cc/100 g of weld metal).

The 10 × 2 × ½ in. (254 × 50.8 × 13 mm) bars were welded using various arc times and weld distances with both low and high-hydrogen practice. After cooling to ambient temperature, the weldments were immediately loaded in the varestraint apparatus (Ref. 7) and a 2% augmented strain was then applied.

During this process, an acoustic-emission transducer was mounted on the specimen surface adjacent to the weld bead, as shown schematically in Fig. 1, to monitor crack initiation and propagation.

Table 2—Summary for Electrodes, Hydrogen Content, Heat Treatments, and Steel Heats Used in Investigation

Diffusible H_2 in welds made with 3/16 in. (4.76) diam. electrodes:	–
Moist E7018[a]	30 ppm
Baked E7018[b]	3 ppm
Heats 32, 27, 1, 0	As-received
Heats 32, 27, 1, 0	Normalized at 1750°F (954°C)
Heat 27	Normalized and postweld heat treatment at 1100°F (593°C)

[a]Electrode dipped in water for 30 seconds.
[b]Electrode stored continuously at 350°F (177°C) after removal from sealed container.

Because of the high ductile-brittle transition temperature (DBTT) of these heats, the hydrogen-induced cracking could not be performed at liquid-nitrogen temperature, −320°F (−196°C).

Specimens were then cut and mounted for metallographic examination and microhardness measurements.

Hydrogen-Induced Cracking Tests

Equations described in an earlier paper (Part I to this paper — Ref. 8) were used to select welding conditions which would give maximum weld heat-affected zone hardness levels ranging from about 25 to 50 Rc in the coarse-grained region at the fusion boundary. Welds were made in heats 32, 27, 1 and 0 using the selected welding procedures to make simulated repair welds with both high- and low-hydrogen practice.

The welded specimens were loaded in the varestraint test apparatus. Then, after attaching the acoustic-emission transducer, they were subjected to a 2% augmented strain for 2 h in order to simulate the mechanical factor by creating yield-strength stresses in the outer fibers of the specimen.

The acoustic-emission data provided qualitative information on the initiation and propagation of hydrogen-induced cracking. However, quantitative correlation between the acoustic-emission counts and the severity of cracking was not found. This was believed at the time to result from extraneous noise in and about the laboratory that caused erroneous counts. However, for reasons that are discussed in a later section, this may be only partially responsible for the lack of correlation.

Fig. 2 — Typical underbead crack in the coarse-grained region of the HAZ of a stationary weld made on heat 27 using high-hydrogen practice. Arc current — 220 A; arc voltage — 25 V; arc time — 5 s; section thickness — ½ in. (12.7 mm); cooling rate at 900°F (482°C) — 49°F/s (27.2°C/s); hardness — 52 Rc (50 Rc predicted). 2% nital, ×500 (reduced 46% on reproduction)

For welds made using high-hydrogen practice the maximum "safe" hardness level was found to be about 33 Rc. Welds made with conditions that produce hardness levels of less than 35 Rc did not exhibit detectable cracks in the coarse-grained region of the heat-affected zone, even with 30 ppm of diffusible hydrogen present.

With low-hydrogen practice, no cracking was detected in the coarse-grained region until hardness levels of approximately 45 Rc were produced.

Figure 2 shows a typical underbead crack, which initiated in the coarse-grained region of the weld heat-affected zone. The microstructure around the crack is predominantly martensitic.

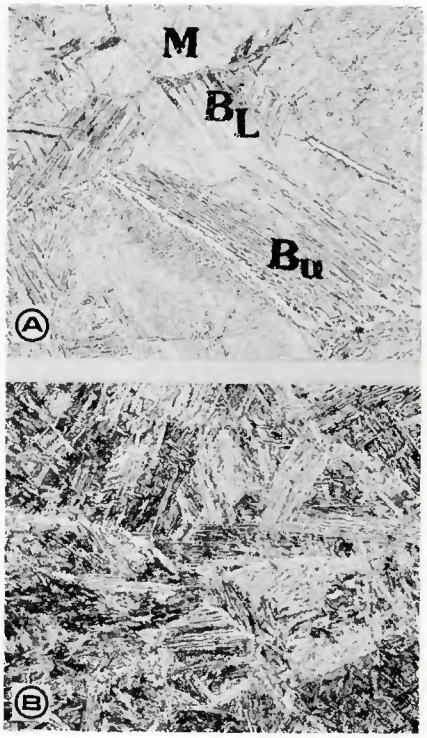

Fig. 3 — Effect of cooling rate on microstructure of repair weld HAZ in heat 1. A — stationary weld (stationary arc); B — linear weld. Welding conditions: for A and B — 220 A arc current, 25 V arc voltage, ½ in. section thickness; for A only — 5 s arc time, cooling rate of 39°F/s @ 900°F, 51 Rc max. hardness; for B only — 10 ipm travel speed, 2.0 in. weld length, 18°F/s cooling rate @ 900°F, 31 Rc max. hardness. 2% nital etch, ×500 (reduced 35% on reproduction)

Figure 3 shows weld heat-affected-zone microstructures which experienced maximum cooling rates of 18 and 39°F/s (10 and 21.7°C/s), respectively, at 900°F (482°C). The structure in Fig. 3A consists of a mixture of martensite (identified by the letter M), lower bainite (identified by the letter B_L) and upper bainite (identified by the letter B_U).

The measured maximum hardness in the martensitic regions of the specimen in Fig. 3A was Rc 51, whereas the calculated value of IH for this material (heat 1) is only 45 Rc. This means that the carbon content of the prior austenite was probably inhomogeneous and was higher than the nominal carbon content in some regions, thus explaining the higher than expected maximum hardness. This is entirely possible because the short time-at-temperature could prevent complete homogenization from occurring even at temperatures just below the solidus. The structure in Fig. 3B consists of upper and lower bainites with maximum hardness level of Rc 31.

The major difference between cast and wrought steel products lies in the nature and severity of the compositional heterogeneity. In both types of product,

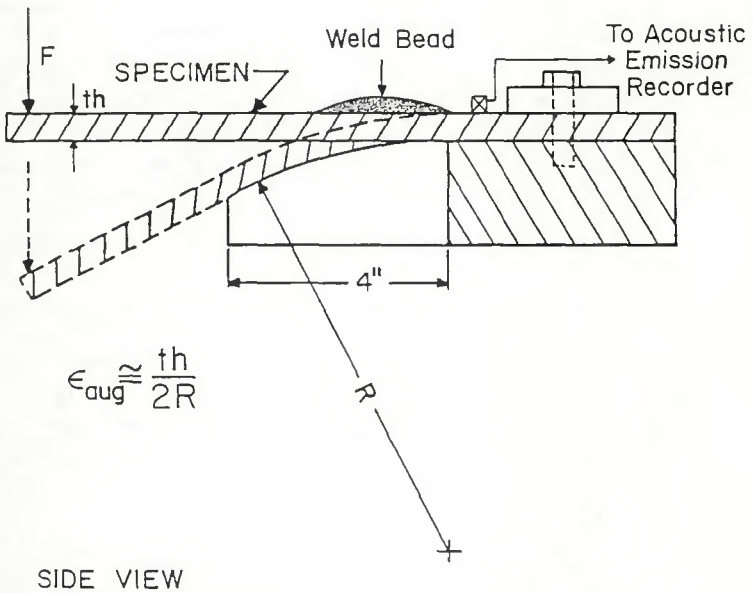

Fig. 1 — Schematic diagram of bending section of the varestraint apparatus and location of acoustic emission transducer with respect to weld

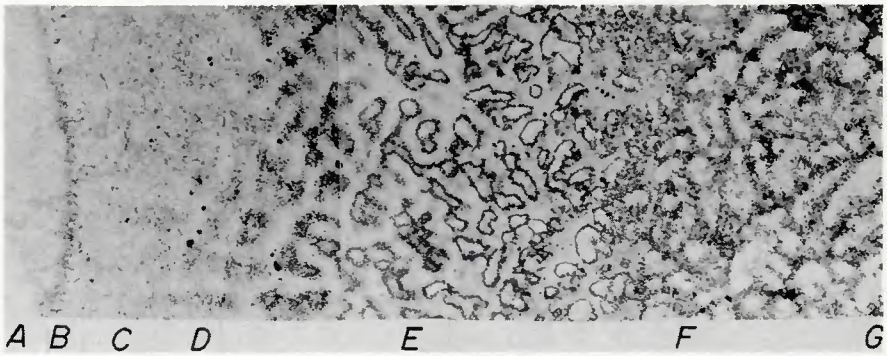

Fig. 4—Microstructure of 5 s stationary repair weld in heat 27 with KHN (50 g load) hardnesses as follows: A—168; B—280; C—403; D—403 prior pearlite, 197 prior ferrite; E—615 prior pearlite, 84 prior ferrite; F—163 prior pearlite; G—(not stated). Nital etch, ×50 (reduced 49% on reproduction)

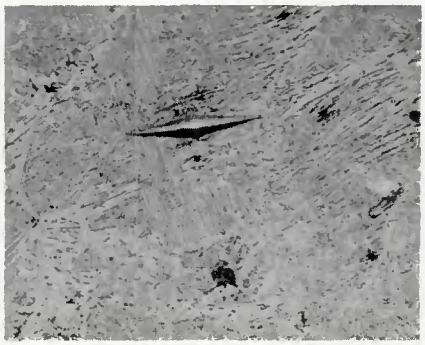

Fig. 5—Region A in Fig. 4 at ×500 (reduced 46% on reproduction). 2% nital etch

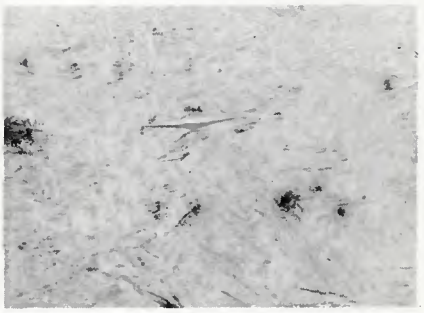

Fig. 6—Region B in Fig. 4 at ×500 (reduced 54% on reproduction). 2% nital etch

the initial solidification process is accompanied by dendritic segregation with the dendrite interstices being enriched in those elements which depress the liquidus temperature of the alloy. However, during soaking at high temperature in preparation for hot-working, partial homogenization occurs, and the pattern of the residual segregation is altered by the hot-working operations. Thus, in the case of hot-rolled plate products, the combination of thermal and mechanical treatment forms alternating bands of solute-rich and solute-lean material parallel to the rolled surface.

In the case of steel castings, the pattern of segregation is controlled by the dendritic-arm spacing, which increases as the section thickness increases. Since no mechanical working is involved, homogenization of castings can only be achieved by diffusion-controlled thermal treatments. When the dendrite-arm spacings are large, the increased diffusion distances require longer times and higher temperatures to achieve a reasonable degree of homogenization. Thus, it is customary to normalize cast steels prior to the final heat-treatment operations which are designed to control the mechanical properties of the castings.

Figure 4 shows the microstructural changes from the fusion zone at the left outward to the unaffected base metal at the right. The panoramic view of the weldment shows seven distinct types of microstructures labelled *A* through *G* in Fig. 4:

A—fusion zone. Figure 5 shows the microstructure of this region as revealed by a 2% nital etch at X500. The microstructure consists of Widmanstätten ferrite and finely laminated pearlite. The hardness of this low-carbon weld metal was only 168 KHN.

B—unmixed zone (Ref. 9). The top section of Fig. 6 shows this zone at X500. Because mechanical mixing is incomplete in this zone, the substitutional alloy content approximates that of the base metal. Carbon, on the other hand, diffuses so rapidly that the carbon content is intermediate between that of the weld (0.07 wt-%) and that of the base metal (0.31 wt-%). The region consists of bainite, Widmanstätten ferrite and very fine pearlite structures with measured hardness of only 280 KHN.

C—homogenized coarsed-grain region. Figure 7 shows the microstructure of this region at X500. The uniform response to the etchant within this region in Fig. 4 indicates it to be reasonably homogeneous as a result of the high peak temperatures experienced in this region. The microstructure is fully martensitic and exhibited a hardness of 403 KHN.

D—inhomogeneous fully transformed region. Within this region the response to the etchant in Fig. 4 is uneven and the mottled appearance is indicative of inhomogeneity. Figure 8 shows a portion of this region at X500. The light gray regions are fully martensitic and exhibited a hardness of 403 KHN. The intermediate regions which consist of a mixture of elevated-temperature transformation products exhibited a hardness of 197 KHN.

Apparently region *D* experienced peak temperatures above the effective A_3 long enough to complete the transformation to austenite but for too short a time to experience homogenization of even the interstitial carbon. The austenite grain size in this region ranges from slightly coarsened to fully refined and the hardenability varies accordingly.

E—partially transformed region (PTR). This region is characterized by regions of nearly eutectoid carbon which correspond to the original networks of pearlite

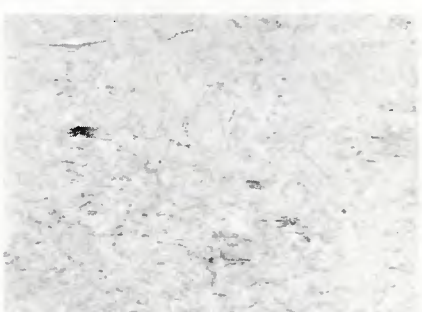

Fig. 7—Region C in Fig. 4 at ×500 (reduced 52% on reproduction)

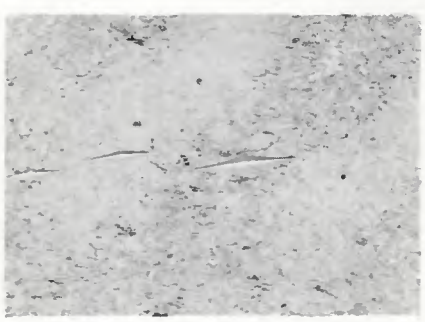

Fig. 8—Region D in Fig. 4 at ×500 (reduced 54% on reproduction). 2% nital etch

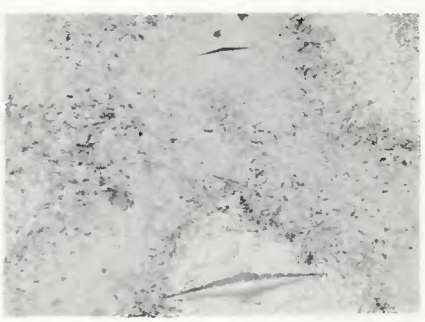

Fig. 9—Region E in Fig. 4 at ×500 (reduced 53% on reproduction). 2% nital etch

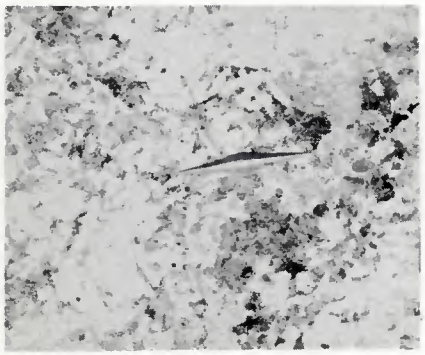

Fig. 10—Region F in Fig. 4 at X500 (reduced 46% on reproduction). 2% nital etch

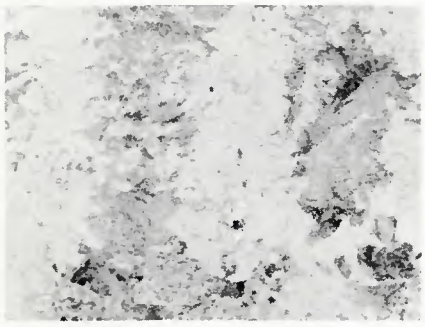

Fig. 11—Region G in Fig. 4 at X500 (reduced 52% on reproduction). 2% nital etch

in the as-cast microstructure. This region transforms to high-carbon austenite whenever the peak temperature exceeds the effective A_1, and the short times-at-temperature prevent significant redistribution of the carbon. Therefore, the continuous prior-pearlite networks form continuous networks of high-carbon austenite; upon cooling, these have sufficient hardenability to transform to continuous networks of high-carbon martensite. The hardness of 615 KHN is in the high-carbon martensitic regions and the low values of 84 KHN are encountered in the

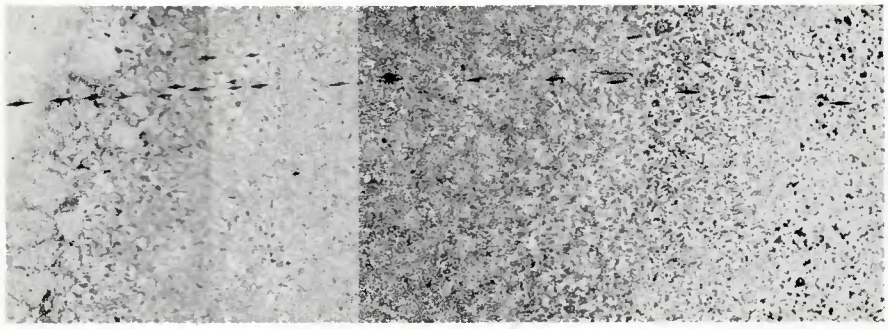

Fig. 14—Microstructure of 5 s stationary repair weld in heat 0. Nital etch, X75 (reduced 42% on reproduction)

untransformed ferrite islands. Figure 9 shows the location of E at X500.

F—spheroidized region. In this region, the peak temperature experienced between the effective A_1 and about 900-1000°F (482-538°C). The lamellar carbides within the pearlite nodules spheroidize while the original ferrite grains remain unchanged. Figure 10 shows this microstructure at X500. The average hardness is 163 KHN in the prior pearlite and about 84 KHN in the prior ferrite.

G—unaffected base metal. This microstructure consists of continuous networks of pearlite nodules at the dendrite interstices as a result of the segregation of carbon and alloying elements to the last material to solidify. This means, in effect, that the as-cast base metal, which has a nominal carbon content of 0.31%, behaves like a composite material. As a composite material, it consists of islands of low carbon ferrite grains (~0.025% C) completely surrounded by nearly continuous networks of material with carbon contents ranging from approximately 0.5% (the carbon content of liquid steel at the peritectic temperature) to nearly eutectoid (~0.8%) composition. Figure 11 shows the microstructure of this zone at X500. Note that the pearlite laminations can be resolved in some areas at this magnification.

Figure 12 summarizes the results of a microhardness traverse across the region shown in Fig. 4. Attention is drawn to the large spread between the maximum and minimum hardness values observed in the partially-transformed region. This reflects the nonuniform carbon content of the martensite formed in this region. Note that the areas of untransformed ferrite in this region exhibited hardness values ranging from 77 to 94 KHN. An approximate scale of Rc hardness is included at the right side of Fig. 12 for comparison with calculated hardness data presented earlier.

Homogenization Studies

The results summarized in the previous section clearly indicate the dangers of repair welding as-cast steel structures. It is

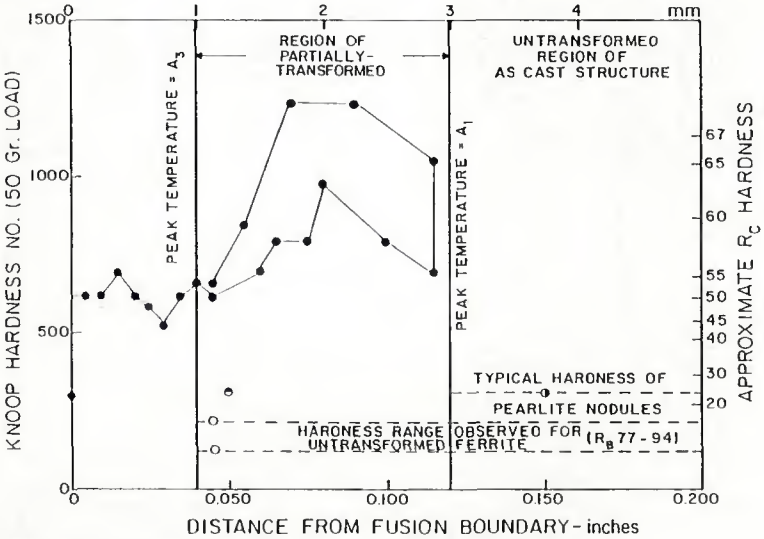

Fig. 12—Results of hardness traverse across regions shown in Fig. 4

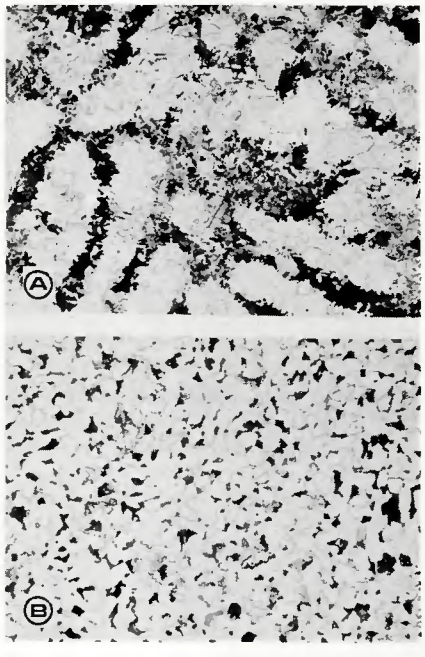

Fig. 13—As-cast and normalized heat 0 microstructures: A—as-cast; B—normalized. 2% nital etch, X250 (reduced 44% on reproduction)

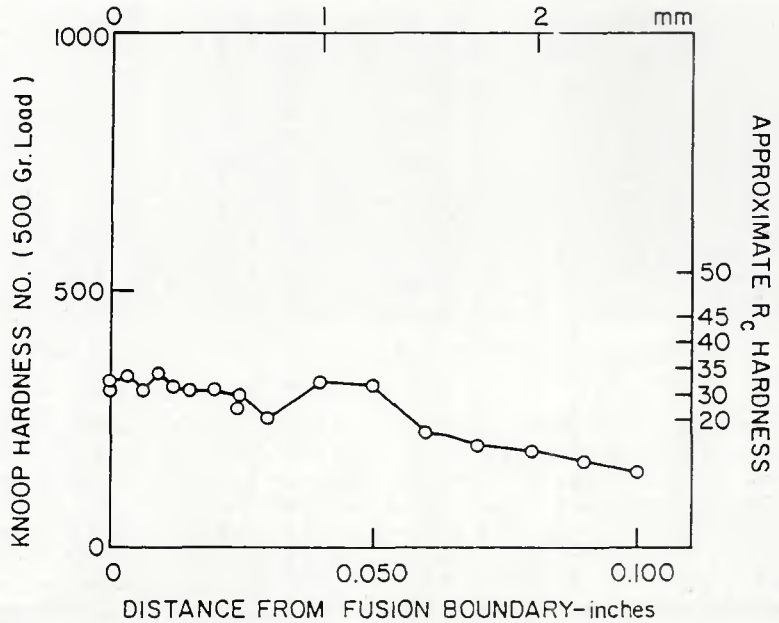

Fig. 15—Results of hardness traverse across the regions in Fig. 14

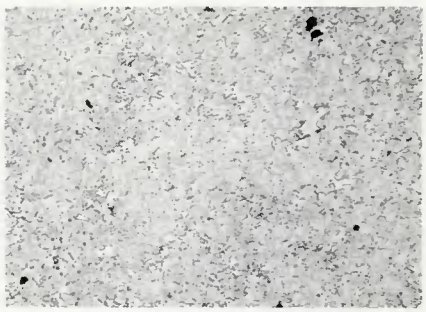

Fig. 18—Tempered martensite in Fig. 17 at X500 (reduced 52% on reproduction). Nital etch

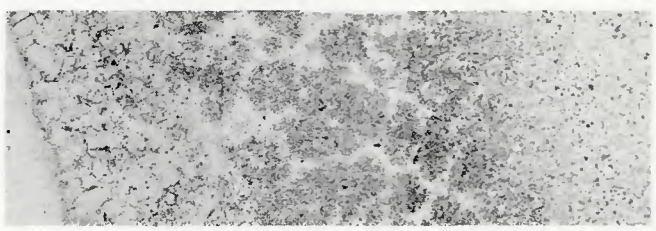

Fig. 16—Microstructure of 5 s stationary repair weld in normalized heat 27. Nital etch, X75 (reduced 55% on reproduction)

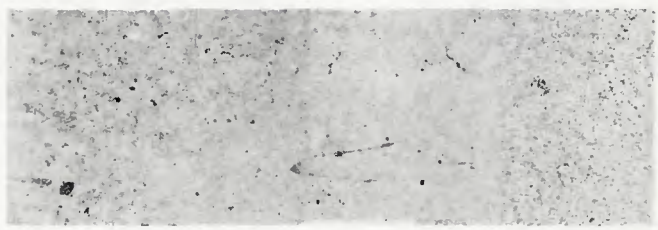

Fig. 17—Microstructure of 5 s stationary repair weld in normalized heat 27 with postweld tempering at 1100°F (593°C) for 1 h. Nital etch, X75 (reduced 55% on reproduction)

virtually impossible to choose welding conditions which provide cooling rates sufficiently slow to prevent the formation of continuous networks of crack-sensitive microstructures in the regions which experience partial transformation to austenite.

The hardness levels identified in these regions are far above those shown to be acceptable for avoiding hydrogen-induced cracking even with good low-hydrogen practice. Thus, it would be difficult, if not impossible, to make repair welds in as-cast steels without the risk of forming microcracks in the high-carbon martensitic networks. In fact, hindsight now suggests that the lack of quantitative correlation between the acoustic-emission studies and identifiable hydrogen-induced cracks is attributable to this phenomenon.

Unfortunately, microcracks in these hard brittle networks in the partially transformed region can serve as nuclei for slow crack growth even after postweld heat treatments. Therefore, it appears that the only sure way to avoid this problem would be to eliminate the networks of interdendritic pearlite nodules by a homogenizing treatment prior to welding. Thus, 10 × 4 × ½ in. (254 × 102 × 13 mm) specimens from each heat were normalized at 1750°F (954°C) for 2 h.

Figure 13 compares the as-cast and normalized microstructures at X250. Note the complete elimination of the continuous networks of pearlite that results from

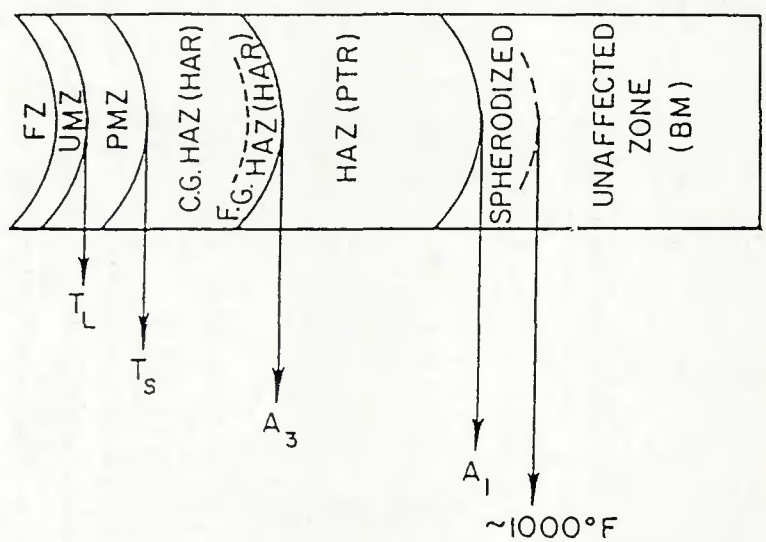

Fig. 19—Schematic of various regions produced in steel casting repair welds: FZ—fusion zone; UMZ—unmixed zone; PMZ—partially melted zone; HAR—homogeneous austenite region; HAZ—heat-affected zone; C.G.—coarse grained; F.G.—fine grained; PTR—partially transformed region

the normalizing treatment.

Figure 14 shows a panorama of a weld made in a normalized specimen from heat 0. Comparison with Fig. 4 indicates that the coarse continuous networks of high carbon martensite have been eliminated by the homogenization treatment. Furthermore, the fine grain size produced by normalizing lowers the hardenability and helps to provide more acceptable microstructures.

Figure 15 is a plot of the microhardness transverse run on the weld shown in Fig. 14. Comparison with Fig. 12 clearly indicates the advantage gained by normalizing. Although these plots are for welds made with identical conditions, the maximum hardness in the normalized material is only about 350 KHN as compared to about 1200 KHN in the weld made in the as-cast material from the same heat.

Figures 16 and 17 show microstructures of welds made in normalized heat 27 with and without a postweld temper at 1100°F (593°C) for 1 h. The weld in Fig. 16 was not tempered and showed some networks of martensite with hardness levels as high as 45 Rc. However, after the postweld temper (Fig. 17), the structures appear more homogeneous, and the region of maximum hardness consists of tempered martensite with a hardness of 40 Rc. Figure 18 shows this same structure at X500.

The various zones, which are produced in the weldment during repair welding of steel castings, are summarized in schematic form in Fig. 19. It is apparent that the region most susceptible to hydrogen-induced cracking is the partially transformed region; here networks of hard and brittle constituents are produced in the inhomogeneous austentite.

It is apparent from the above results that a normalizing treatment should precede any repair weld of steel castings if the danger of hydrogen-induced cracking is to be minimized. In general, with increases in both the alloying content and the section thickness, the segregation becomes more severe and ultimately a postweld heat tempering will become necessary.

Conclusions

The following conclusions pertain to the hydrogen-induced cracking studies of repair welds in steel castings.

1. The metallurgical factor was controlled by using the method described previously to select combinations of welding conditions which produced both crack-sensitive and crack-insensitive microstructures in typical case steel specimens.

2. The chemical factor was controlled by modifying the moisture content of the E7018 electrode coatings.

3. The mechanical factor was synthesized by applying a controlled augmented strain to SMA welds deposited on simple rectangular specimens.

4. Acoustic-emission techniques were employed to monitor the initiation and growth of hydrogen-induced cracking.

5. The results confirm the fact that proper low-hydrogen practice is mandatory for all repair welding operations if hydrogen-induced cracking in the coarse-grained heat-affected-zone is to be avoided.

6. The susceptibility to hydrogen-induced cracking is directly related to both the maximum hardness in the heat-affected zone and the level of diffusible hydrogen.

7. Hydrogen-induced cracking can be prevented by using good low-hydrogen practice if the maximum hardness in the heat-affected zone is kept below Rc 35.

8. Since the maximum hardness in the heat-affected zone is directly related to the carbon content, reduction in the carbon content is the simplest way to improve the weldability of steel castings.

The following conclusions pertain to the results of microstructural studies of repair welds in steel castings:

1. For cast steel repair welds one can identify seven distinct regions by a nital etch.

2. The partially-transformed region of the heat-affected zone of repair welds in as-cast steel was found to have the microstructure most susceptible to hydrogen-induced cracking.

3. Continuous networks with hardness levels ranging from 600 to 1200 KHN (50 to 70 Rc) were identified in the partially-transformed region.

4. The problem in the partially-transformed region arises from the interdendritic segregation present in the as-cast material.

5. Normalizing eliminates the problem in the partially-transformed region by homogenization.

6. All steel castings should be normalized before repair welding to minimize problems in the partially-transformed region.

7. As the alloy content is increased, postweld-heat treatment may become desirable.

Acknowledgments

The authors wish to thank Mr. Dan Stone and the Association of American Railroads (AAR) for its financial support of this project.

References

1. Rogers, H. C. 1956. The influence of hydrogen on the yield point in iron. *Acta Met.* 4(2):114-117.

2. Savage, W. F., Nippes, E. F., and Homma, H. 1976. Hydrogen-induced cracking in HY-80 steel weldments. *Welding Journal* 55(11):368-s to 376-s.

3. Frohmberg, R. P., Barnett, W. J., and Troiano, A. R. 1955. Delayed failure and hydrogen embrittlement in steel. *Trans. ASM* 47:892.

4. Adams, C. M., Jr. 1958. Cooling rates and peak temperatures in fusion welding. *Welding Journal* 37(5):210-s to 215-s.

5. Savage, W. F., Nippes, E. F., and Szekeres, E. S. 1976. Hydrogen-induced cold cracking in a low-alloy steel. *Welding Journal* 55(9):276-s to 283-s.

6. Ball, D. J., Gestal, W. J., Jr., and Nippes, E. F. 1981. Determination of diffusible hydrogen in weldments by the RPI silicone-oil extraction method. *Welding Journal* 60(3):50-s to 56-s.

7. Savage, W. F., and Lundin, C. D. 1965. The varestraint test. *Welding Journal* 44(10):433-s to 442-s.

8. Aidun, D. K., and Savage, W. F. 1984. Optimizing repair welding techniques in cast steels – Part I. *Welding Journal* 63(11):345-s to 353-s.

9. Savage, W. F., Nippes, E. F., and Szekeres, E. S. 1976. A study of weld interface phenomena in a low alloy steel. *Welding Journal* 55(9):260-s to 268-s.